Egyptian Journal of Aquatic Biology & Fisheries
Zoology Department, Faculty of Science,
Ain Shams University, Cairo, Egypt.
ISSN 1110 – 6131
Vol. 28(5): 2001 – 2018 (2024)
www.ejabf.journals.ekb.eg

Retina of Fantail and Black Moor Strains of the Goldfish (*Carassius auratus*) with Their Molecular Identification

Ahmad M. Azab[1*], Walaa Shalaby[2], Mohamed A. M. El Tabakh[1], Sanaa E. Abdel Samei[2], Mohamed M. A. Abumandour[3], Doaa Gewily[2]

[1]Zoology Department, Faculty of Science (Boys), Al-Azhar University, Cairo, Egypt
[2]Zoology Department, Faculty of Science (Girls), Al-Azhar University, Cairo, Egypt
[3]Department of Anatomy and Embryology, Faculty of Veterinary Medicine, Alexandria University, Alexandria, Egypt

***Corresponding author:** amazab2000@yahoo.com

ARTICLE INFO
Article History:
Received: Oct. 4, 2024
Accepted: Oct. 23, 2024
Online: Oct. 30, 2024

Keywords:
Carassius auratus,
Black Moor goldfish,
Fantail goldfish,
Bioinformatic analysis,
Cone photoreceptors,
Transmission electron microscopy (TEM)

ABSTRACT

The present study was conducted to investigate the morphological features of the retinal photoreceptors of two goldfish strains: the black moor and fantail, using light (LM) and transmission electron microscopy (TEM) to illustrate their visual adaptation to the fish's lifestyle. Both the fantail and black moor have been DNA barcoded using COI partial sequence and proved to belong to *Carassius auratus* species. The newly obtained sequences were banked to the gene bank and given accession numbers: PP106365 and PP106366, respectively. Histologically, both strains had the same retinal characteristics as all vertebrates. The retina consists of a pigmented epithelium on the exterior and a neural layer with many layers within. Both strains possessed cone photoreceptor cells exclusively, which suggested that their visual adaptation was related to their watery habitat. Significant changes in the arrangement of photoreceptors and the thickness of the retinal layer between both strains imply that visual acuity and color perception may differ due to their adaptations to distinct ecological niches. Through TEM, the cone cells were observed, providing comprehensive information about their structural specializations that allow them to efficiently absorb and convert light. Our research highlights species-specific discrepancies in the thickness of different retinal layers, hence emphasizing the existence of unique visual processing capacities. The present work enhanced the understanding of *Carassius auratus'* evolutionary biology and the intricate nature of visual adaptations, which are crucial for understanding fish vision and the evolutionary forces shaping their sensory systems in their surroundings.

INTRODUCTION

The fantail, a freshwater goldfish characterized by its egg-shaped body, extended dorsal fin, long quadruple tail fin, and lack of a shoulder hump, serves as the foundation for numerous fancy goldfish species. The black moor, a black variant of the telescope goldfish with protruding eyes, is also known as black moors, blackamoors, or moors—terms that refer to the black North African Muslim inhabitants of Al-Andalus. Both the fantail and black moor goldfish belong to the species *Carassius auratus*, the genus *Carassius*, and the family Cyprinidae within the order Cypriniformes. These two fish are commonly kept as pets in

indoor aquariums and are among the most popular aquarium fish **(Skomal, 1996)**. The eye, being a vital sensory organ, serves an exceptionally critical function in facilitating communication between organisms and their environment **(Kassab *et al.*, 2001; Azab *et al.*, 2017; Aboelnour *et al.*, 2020; Bassuoni *et al.*, 2021; Peter-Ajuzie *et al.*, 2021)**. Numerous eye characteristics of vertebrates are adaptations to the visual environments in which they have evolved **(Land & Nilsson, 2002)**. Eye size varies greatly across vertebrates and is tightly linked to visual abilities. Large eyes confer either greater visual acuity, greater light sensitivity, or a combination of both. Eyes reproduce images on the retina to provide an accessible code for further visual information processing **(Zeigler & Bischof, 1993)**. Therefore, in addition to eye size and lens diameter, additional parameters include the angular spacing of the receptors, the quality of the optic components, and the spacing between ganglion cells impacting visual acuity **(Zeigler & Bischof, 1993; Veilleux & Kirk, 2014)**. A longer focal length, which controls the size of the retinal area where an object's image expands, is possible with larger eyes **(Veilleux & Kirk, 2014)**. There is a correlation between this particular eye shape and enhanced spatial resolution. Due to the fact that focal length influences the area of the retina over which the image is dispersed, an enlargement of this dimension causes the image to appear more magnified on the retina **(Veilleux & Kirk, 2014)**. Fish are equipped with a diverse array of sensory organs that enable them to perceive and interpret a wide variety of environmental stimuli. The size and position of the eye, the morphology and structure of the pigment epithelium, and the structure of the retinal photoreceptors all influence fish vision **(Levine & MacNichol, 1982; Fishelson *et al.*, 2004)**.

The retina is made of two distinct layers: a pigmented layer, which is comprised of a solitary row of cuboidal epithelium, and nine neural layers containing photoreceptors (rods and cones) and different neurons **(Ptito *et al.*, 2021)**. Retinal photoreceptors are cells that are highly polarized and highly specialized **(Braekevelt, 1994; Abumandour *et al.*, 2021; Abumandour *et al.*, 2022a; Elghoul *et al.*, 2022; Gewily *et al.*, 2024; Kandyle *et al.*, 2022)**. A non-motile joined cilium connects the outer segment (light-sensitive region) to the inner segment (synthetic region); the photoreceptor also has a nuclear region and a synaptic termination **(Braekevelt, 1994)**. Retinal photoreceptors have been categorized as either rods or cones according to their light microscopic morphological characteristics. Photoreceptors in the outer nuclear layer sense light and transmit visually evoked signals to interneurons in the inner nuclear layer; the interneurons (horizontal cells, bipolar cells, and amacrine cells) process the information and supply it to retinal ganglion cells (RGCs) in the innermost layer, and the RGCs send axons through the optic nerve to visual centers in the brain **(Masland, 2012; Sanes & Masland, 2015; Zeng & Sanes, 2017; Shekhar *et al.*, 2023)**. The changes in retinal structure between species are indicative of the photic environmental circumstances and eating patterns of each species. In low-light conditions, rod cells are utilized to achieve high visual sensitivity. In contrast, cone cells offer superior spatial and temporal resolution compared to rod cells and enable color vision through the comparison of absorbance across various cone types that are more sensitive to specific wavelengths **(Kondrashev *et al.*, 2023)**.

The current study was prepared to investigate the structure of the retina photoreceptors in two goldfishs: Fantail and Black Moor, using light microscopy (LM) and transmission electron microscopy as an attempt to visual adaptation by their different shapes

and sizes of eye. This study helps understand the retina's morphology and relationship to the fish's lifestyle. Our findings are the outcomes of comparing photoreceptor structures in two goldfish species to understand how eye shapes and sizes affect visual acuity and behavior, potentially revealing insights into aquatic animal vision evolution.

MATERIALS AND METHODS

1. Experimental samples' collection

The current study was conducted on twenty fish specimens from both black moor and fantail goldfish in good condition (Fig. 1A, C). They were collected from the private ornamental fish market. Within two hours, all fish were moved in a 10-gallon glass aquarium with aerated water and temperatures between 18 and 20ºC at the laboratory of Marine Biology, Zoology Department, Faculty of Science, Al-Azhar University, Cairo, Egypt. All the gathered fish were free of any anatomical abnormalities. The anatomical nomenclature was applied according to **Baumel *et al*. (1993)**.

They were euthanized using benzocaine (4mg/ L) according to standard commercial fishing conditions **(Bolasina *et al*., 2017)**, followed by cervical dislocation that was carried out by an experienced veterinary surgeon in accordance with local, national, and international ethics guidelines, and examined for any anatomical abnormalities, especially in the eye. Benzocaine (ethyl 4-aminobenzoate 99%, Sigma Aldrich Co., USA), prepared a few minutes before experiments, was dissolved in ethanol due to its limited ability to dissolve in water, as it is an essential ingredient in the experiments. The fish were grossly examined on four fish, microscopically using light on four fish, and by scanning electron microscopy (SEM) on four fish. The collected fish followed the guidelines established for the 'Sampling protocol for the pilot collection of catch, effort, and biological data in Egypt' **(Dimech *et al*., 2012)**.

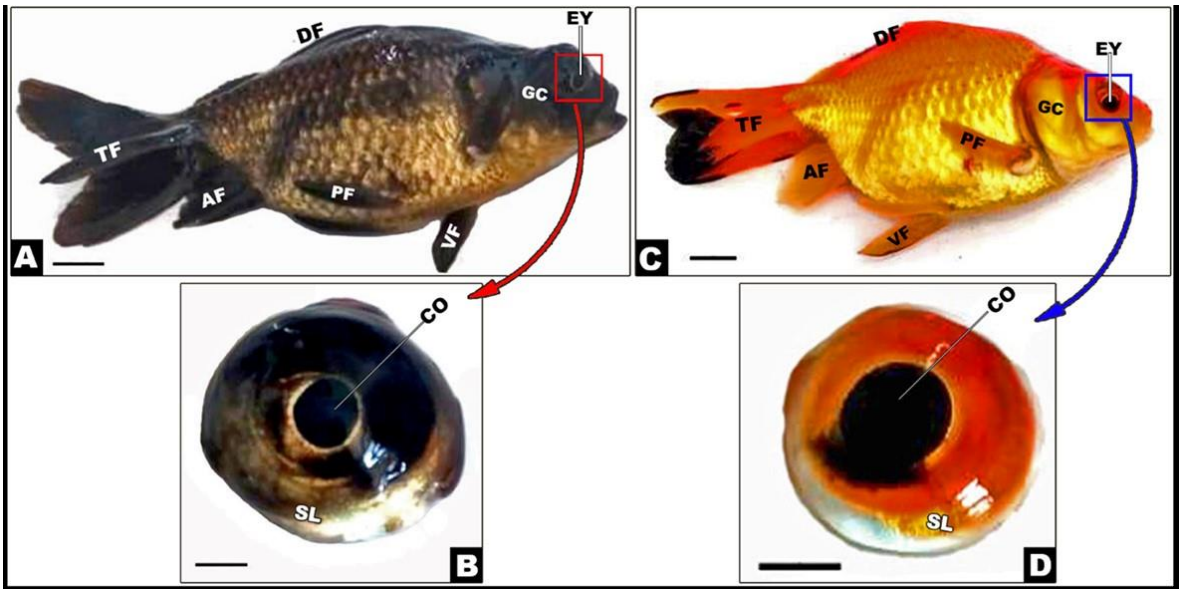

Fig. 1. (A) Gross anatomy of the black moor goldfish **(B)** with its isolated eye and **(C) the** fantail goldfish **(D)** with its isolated eye showing: fish parts such as the dorsal (**DF**), anal (**AF**), pectoral (**PF**), pelvic (**VF**), and tail fin (**TF**); the external layers of eye; the rostral cornea (**CO**) and the caudal large sclera (**SL**). (Scale bar of "view A and C" equal to 5mm; and scale bar of "view B and D" equal to 2mm).

2. DNA extraction and analyses

Tissue subsamples were isolated from the muscle tissue of the collected specimens and were preserved in 100% ethyl alcohol and refrigerated at -20°C. Using the DNeasy Tissue Kit (QIAGEN), DNA was extracted from the tissue according to the manufacturer's instructions. Using newly designed primers, 679bp were amplified from the 50 regions of the cox1 gene from mitochondrial DNA **(Ward *et al.*, 2005)**:

FishF1-50TCAACCAACCACAAAGACATTGGCAC30,

FishR1-50TAGACTTCTGGGTGGCCAAAGAATCA30

PCR reaction mixes consist of 5µL of extracted genomic DNA, 12.5µL of green master mix, 1µL forward primer, and 1µL reverse primer. The experimentation was conducted utilizing a Master Cycler Eppendorf gradient thermal cycler. Commencing with a 2-minute increment at 95°C, the thermal profile proceeded through 35 cycles consisting of the following: 0.5 minutes at 94°C, 0.5 minutes at 54°C, and 1 minute at 72°C; 10 minutes at 72°C; and 5°C. Following examination on 1% agarose gels, the most robust PCR outcomes were selected for sequencing. At an Egyptian genetic center, the PCR product underwent two-directional sequencing (Color Laboratory Co.). The amplified DNA was observed on a 1% agarose gel that had been stained with ethidium bromide, employing a transilluminator, in order to evaluate the PCR reaction's quality and yield (U.V. transilluminator, Spectro-line, Westbury, USA).

3. Bioinformatic analysis

The assembled sequences were processed utilizing the Chromas Pro 1.5 beta software (Technelysium Pty., Tewantin, QLD, Australia). A basic local alignment search tool (BLAST) was utilized to compare the recently obtained *Carassius auratus* COI sequences (PP106365 and PP106366) with sequences already present in GenBank. The BLAST interface is accessible at http://blast.ncbi.nlm.nih.gov/Blast.cgi. For sequence alignment, the MUSCLE algorithm, developed in the MEGA 11.0 program, was applied. Sequence divergences were computed using the Tamura model with three parameters **(Tamura, 1992)**. To visualize species divergence patterns, neighbor-joining (N.J.) trees were generated with the Tamura 3-parameter method **(Tamura, 1992)**. Bootstrapping was conducted in MEGA 11.0 with 1,000 replications, following the methodology described by **Kumar *et al.* (2004)**. The resulting data were further enhanced using iTOL software for visualization **(Letunic & Bork, 2021)**.

4. Eye shape

Each eyeball was cleaned of all fascia and extra-ocular muscles before being inflated by injecting a small amount of formaldehyde in 0.1 M with a syringe and small-gauge needle **(Hall & Ross, 2007; Peter-Ajuzie *et al.*, 2021)**. The fixative was injected into the eyeball until it was fully inflated and would not accept any more liquid (Fig. 1B, D). All fish eyes could be fully inflated and so were used for subsequent measurements. The maximum eye diameter (ED) and the maximum axial length (AL) of each eyeball were measured to 0.1mm using digital calipers. These values were transformed to the logarithm ($\log_{10}$) values to calculate the eye shape ratio according to **Hall and Ross (2007)** applying the following equation:

$$\textbf{Eye shape} = \log_{10}\{ED / AL\}$$

5. Histological investigations

In order to conduct light microscopic examinations, three eyeball specimens from each of the goldfish under investigation were preserved in Bouin's solution for four hours, sectioned at $^{1}/_{3}$ and $^{2}/_{3}$ using a cross-sectional acute scalpel, and then immersed in Bouin's solution for ten hours at room temperature **(Bassuoni *et al*., 2021; Peter-Ajuzie *et al*., 2021)**. Subsequently, the specimens were rinsed for twenty-four hours with 70% ethyl alcohol, dehydrated in ascending grades of ethyl alcohol, cleared in xylene, and encapsulated in molten paraffin wax at 58–62ºC **(Abumandour *et al*., 2022b)**. Following this step, the paraffin blocks were sectioned at a thickness of 5µm with a Leica rotatory microtome (RM 20352035; Leica Microsystems, Wetzlar, Germany) in accordance with the guidelines of **Suvarna *et al*. (2013)**. Then, the sections were stained with hematoxylin and eosin "H&E". The selected sections were examined with a light BX50/BXFLA microscope (Olympus, Tokyo, Japan), and photographed with an U3cmos14000Kpa (USB2.0) model, with a camera used to take the photos for examination of the general histology.

6. Transmission electron microscopy investigations

In order to perform transmission electron microscopy, each eye was immediately severed from orbit by halving it. The retina was meticulously extracted from the eyecup and, using forceps, it was separated from the choroid and vitreous body **(Aboelnour *et al*., 2020)**. Each retina was then sectioned into small pieces and was fixed for approximately five hours in a solution of 0.1 M cacodylate buffer containing 2.5% glutaraldehyde in phosphate buffer (pH 7.4). Subsequently, the sections were rinsed in phosphate buffer (pH 7.4) and post-fixed in buffered 1% osmium tetroxide. Following a thorough rinsing in buffer, the specimens were dehydrated in a succession of cold ethyl alcohol in ascending order, cleaned in propylene oxide, and mounted in epoxy resin **(Hayat, 1986)**. Leica Ultracut UCT microtome was utilized to cut ultrathin slices, which were then put on grids, stained with lead citrate and uranyl acetate, and analyzed with a JEOL 1010 transmission electron microscope.

7. Morphometric measurements of retina

Equipped with a linear ocular micrometer, the thickness of the whole retina and its layers was determined in the goldfish under investigation. A method was employed to investigate the ratio of the relationship between the outer and inner nuclear layers according to **Wang *et al*. (2011)** and **Darwish *et al*. (2015)** to determine the different patterns of eye shapes of the goldfishes.

RESULTS

1. Molecular investigation

Using the neighbor-joining technique, the evolutionary history was deduced. As shown in Fig. (2), the optimum tree depicts the interrelationships between taxa. As established by the bootstrap test (1000 repetitions), the branches inside the tree correspond to the proportion of replicate trees in which the linked taxa grouped. The evolutionary distances were determined with the Tamura 3-parameter approach, wherein the lengths of the branches

correspond to the number of base substitutions per site. The tree is depicted on a scale. All unclear sites were eliminated via pairwise deletion from the nine nucleotide sequences that comprised the analysis. 495 locations were included in the final dataset.

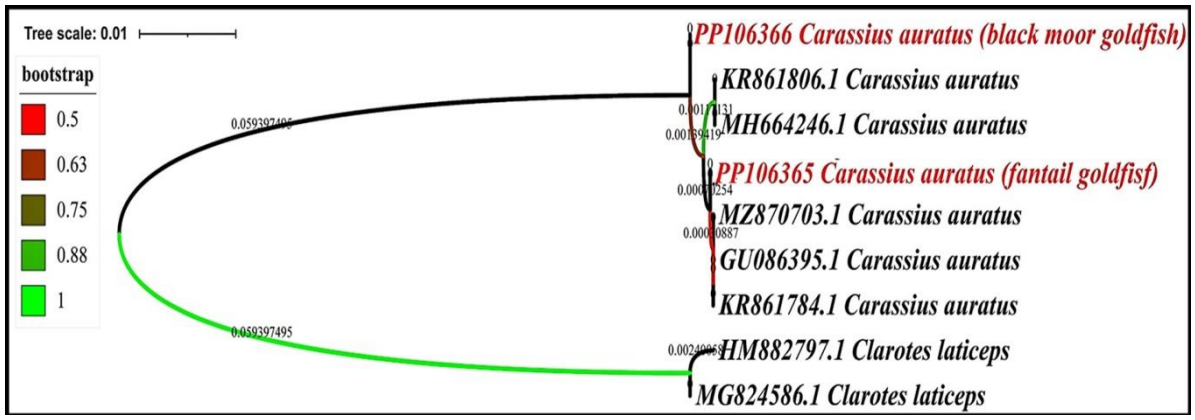

Fig. 2. Evolutionary phylogenetic analysis by neighbor-joining method

2. Eye shape

Our findings illustrate the relationship between eye diameter (ED) and axial length (AL) of the eye. Eye shape measurements of the black moor and fantail goldfish are presented in Table (1). The findings showed that eye diameter (ED) in the black moor goldfish is larger (15.8 ± 3.62mm) than that of the fantail (8.4 ± 1.96mm). The axial length (AL) in the black moor is longer (10.6 ± 2.68mm) than that of the fantail (4.2 ± 0.98mm). Moreover, the ratios of ED and AL with head length (HL) had higher values in the black moor than those recorded in the fantail goldfish. All measurements and ratios were highly significant and varied between the studied goldfish.

Table 1. Eye measurements and shape in relation to body measurements (mm) of the black moor and fantail goldfish

Measurements	Black moor		Fantail		*P*-value
	Range	Average ± SD	Range	Average ± SD	
TL (mm)	80.5 - 161	120.8 ± 28.17	84.0 - 168.0	126.0 ± 29.39	N.S.
HL (mm)	21.0 - 40.0	31.5 ±7.58	24.0 – 50.0	37.3 ± 9.10	P<0.01
HL/TL (%)	23.9 - 27.7	26.1 ± 1.34	28.1 – 30.8	29.5 ± 0.94	P< 0.001
ED (mm)	10.5 - 21.0	15.8 ± 3.62	5.6 – 11.2	8.4 ± 1.96	P< 0.001
ED/HL (%)	47.1 - 54.5	50.2 ± 2.62	21.6 – 23.7	22.6 ± 0.72	P< 0.001
AL (mm)	7.0 - 14.5	10.6 ± 2.68	2.8 – 5.6	4.2 ± 0.98	P< 0.001
AL/HL (%)	31.6 - 34.5	33.7 ± 1.45	10.8 – 11.9	11.3 ± 0.36	P< 0.001
Log_{10}(ED/AL)	**0.14: 0.20**	**0.173 ± 0.018**	**0.29: 0.33**	**0.302 ± 0.017**	**P< 0.001**

AL: Axial length of eye; **ED**: Eye diameter; **HL**: Head length; **TL**: Total length.

3. Histological investigation of retina

The findings of the retina of the two goldfish revealed that its structure resembles that of other vertebrate retinas. The structure comprises two primary strata: the innermost is the neural layer, which is composed of nine strata: the photoreceptor cell layer (PL), which was exclusive to both fish species and was composed of cones; the external limiting membrane (OLM); the external nuclear layer (ONL); the external plexiform layer (OPL); the internal

nuclear layer (INL); the internal plexiform layer (IPL); the ganglion cell layer (GCL); the nerve fiber layer (NFL); and the innermost which is the pigmented epithelium (PE) (ILM) (Fig. 3).

The external layer appeared brown due to their inclusion of melanin granules. The external layer is composed of a single layer of epithelial cells called the pigmented epithelium, which extends outward to the photoreceptor layer to support this layer as well as to absorb the scattered light passing through these cells. In the black moor goldfish, the external pigmented epithelium layer is distributed in the peripheral region of the photoreceptor layer with a thick, dense layer, while in the fantail goldfish, it is distributed in the epithelial cells with a much larger and thicker layer covering the largest part of the photoreceptor layer (Fig. 3B, D).

The photoreceptor layer has only one type of photoreceptor cell: the cone cells, which are linked outside with the pigmented epithelium. In both the black moor and fantail goldfish, the visual cell layer is composed of single- cone and double- cone cells. In the black moor goldfish, the cones are scattered along this layer, while in the fantail goldfish, they are more condensed and much larger than those in the black moor (Fig. 3B, D).

In both the black moor and fantail goldfish, the outer limiting membranes were clear, a light layer appeared in all areas, and the photoreceptor layer is separated from the external nuclear layer. The external nuclear layer (ENL) is composed of the visual cell bodies; the thickness of this layer varied between the two studied species. In the black moor goldfish, the number of rows of cells is between 4 and 5 in a scattered pattern, while in the fantail goldfish, the number of rows is between 3 and 4 in a more condensed pattern than in black moor goldfish. The external plexiform layer (EPL) thickness in the two studied species varied from each other. In the black moor goldfish, the layer is wide with densities of both bipolar and horizontal cells, whereas in the fantail goldfish, this layer is narrow and is linked with the axons of the visual cells and the densities of both bipolar and horizontal cells (Fig. 3B, D).

The internal nuclear layer (INL) is distinguished by its heterogeneous cell composition, which included both bipolar and horizontal cells. The thickness of this layer differed between the two examined fish. In contrast, this layer is more compressed in the fantail goldfish, where the number of rows varies from one to two, whereas in the black moor goldfish, it is extremely dispersed and ranges from four to five. The external plexiform layer (EPL) thickness is greater than the internal plexiform layer (IPL) thickness in both examined fish strains (EPL). Interlocking dendrites of ganglion cells and axes of bipolar cells constitute this layer, which constituted a single stratum of ganglion cells. Ganglion cell (GCL) axons assemble to create the nerve fiber layer (NFL), which became denser as it approached the optic nerve, which was originated from the eye, and ultimately connected to the brain. The thickness of the optic nerve fiber layer varied between the two species. It is a foundation plate composed of muller cells and served as the inner limiting membrane separating the vitreous humor from the retina (Fig. 3B, D).

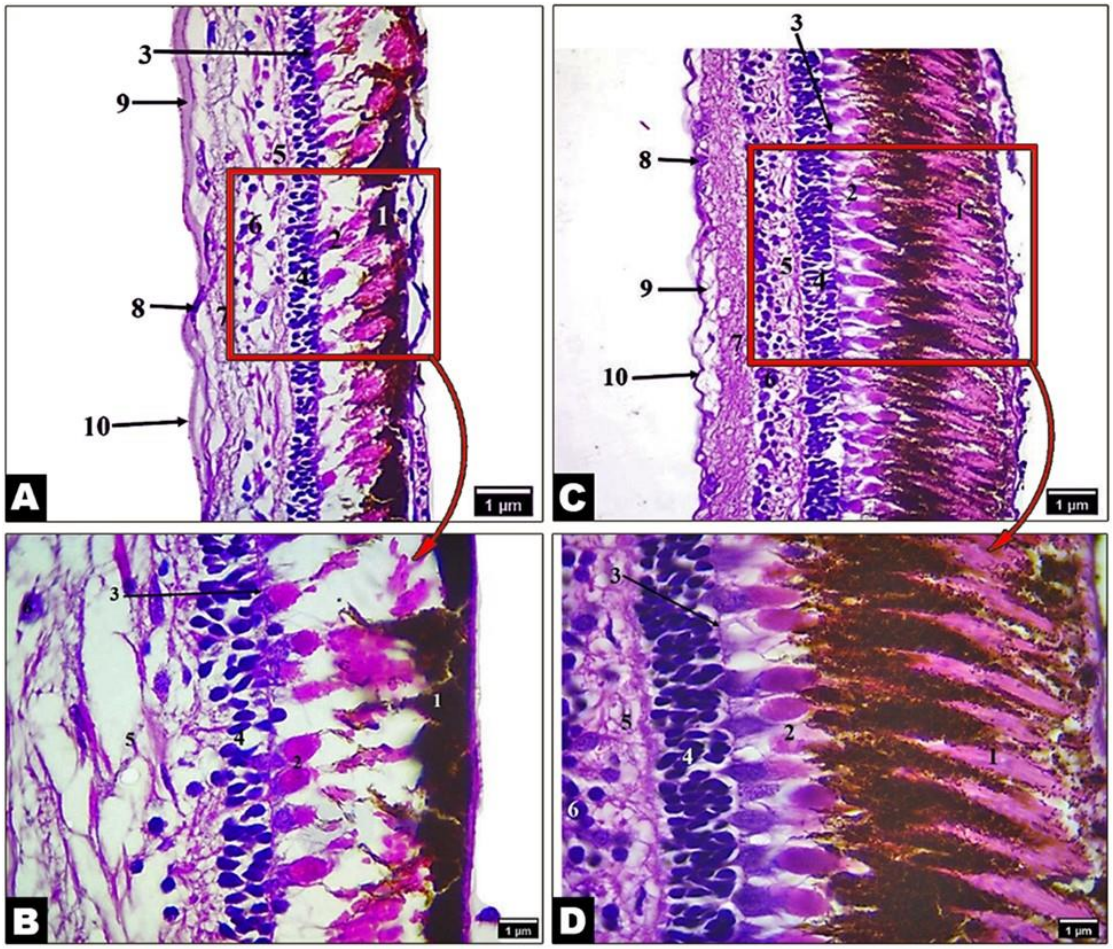

Fig. 3. A photomicrograph of the retina in the black moor goldfish (Views **A** and **B**) and the fantail goldfish (Views **C** and **D**) showing layers of retina; **1.** Pigmented epithelium; **2.** Photoreceptor layer; **3.** Outer limiting membrane; **4.** Outer nuclear layer; **5.** Outer plexiform layer; **6.** Inner nuclear layer; **7.** Inner plexiform layer; **8.** Ganglion layer; **9.** Nerve fiber layer; and **10.** Inner limiting membrane

4. Morphometric measurements of retinal layers

There was a great variation that appeared between the two examined goldfish in the thickness of the different retinal layers (Table 2). The thickness of the total retinal layer in the fantail was longer (215.4 ± 7.18µ) than that found in the black moor (125.4 ± 10.46µ) goldfish. The thickness of the pigmented epithelium layer in the black moor was less thick (17.10 ± 6.68µ) than that in the fantail goldfish, which recorded 59.08 ± 2.77µ. The thickness of the photoreceptor layer in the black moor was clearly reduced (47.05 ± 8.57µ) than that in the fantail, which was considerably thicker, with an average of 81.1±3.83µ. The thickness of the outer nuclear layer in the black moor (15.3 ±3.09µ) was less than those in the fantail (17.4 ±0.97µ). The thickness of the inner nuclear layer in the black moor (17.42 ± 5.68µ) was larger than those in the fantail (15.5 ±2.35µ). The thickness of the outer plexiform layer and the inner plexiform layer in the black moor (8.02 ± 2.30 and 11.79 ± 4.03µ, respectively) were reduced comparing with those observed in the fantail (10.6 ±2.32 and 20.4 ±1.70µ). The thickness values of the total retina and different neural retinal layers were significantly varied between the black moor and fantail goldfish (Table 2).

Table 2. Thickness (μ) of some neural retinal layers of the black moor and fantail goldfish

Retinal layer	Black moor		Fantail		*P*-value
	Range	Average ± SD	Range	Average ± SD	
RL	108.9 – 143.4	125.4 ± 10.46	203.7- 228.1	215.4 ± 7.18	*P*< 0.001
PE	8.92 – 26.67	17.10 ± 6.68	54.27 – 65.10	59.08 ± 2.77	*P*< 0.001
PHL	32.02 – 62.99	47.05 ± 8.57	74.54 – 89.34	81.10 ± 3.83	*P*< 0.001
ONL	9.45 – 24.20	15.29 ± 3.09	15.78 – 18.90	17.36 ± 0.97	*P*> 0.05
OPL	3.15 – 11.07	8.02 ± 2.30	7.35 – 13.69	10.63 ± 2.32	*P*> 0.05
INL	10.50 – 33.61	17.42 ± 5.68	9.97 – 18.96	15.50 ± 2.35	*P*> 0.05
IPL	7.42 – 20.01	11.79 ± 4.03	17.33 – 23.63	20.38 ± 1.70	*P*< 0.001

RL: Retinal layer total thickness; **PE:** Pigment epithelium; **PHL:** Photoreceptor layer; **ONL:** Outer nuclear layer; **OPL:** Outer plexiform layer; **INL:** Inner nuclear layer; **IPL:** Inner plexiform layer.

5. Transmission electron microscopy (TEM) investigation of retina

The photoreceptor layer of the retina in both the black moor goldfish and fantail goldfish had only the cone-type of photoreceptors. The cone comprised a single cone and a double cone. The double cone is composed of a chief cone and an accessory cone. Both the single and double- cone cells consisted of an outer segment and an inner segment (Figs. 4, 5). The outer segments were closely associated with the pigment epithelial cells, and they were tall, wide, and occupied by a membrane as flattened sacs. The inner segments were very wide and densely packed with mitochondria in their ellipsoid region (Figs. 4, 5).

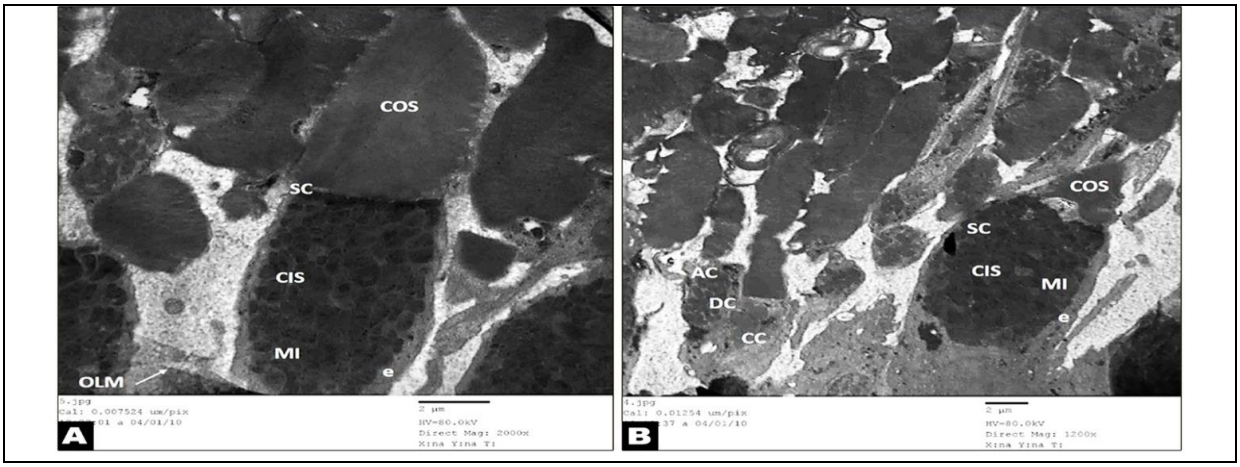

Fig. 4. Transmission electron microscopic micrographs of the retinal photoreceptor layer of Black Moor goldfish showing: Single cone **(SC)**; Double cone **(DC)**; Ellipsoid region **(e)**; Mitochondria **(Mi)**; Outer limiting membrane **(OLM)**; Cone outer segment **(COS)**; Cone inner segment **(CIS)**; Chief Cone (**CC)** and Accessory cone (**AC)**. (A: X 2000 and B: X 1200)

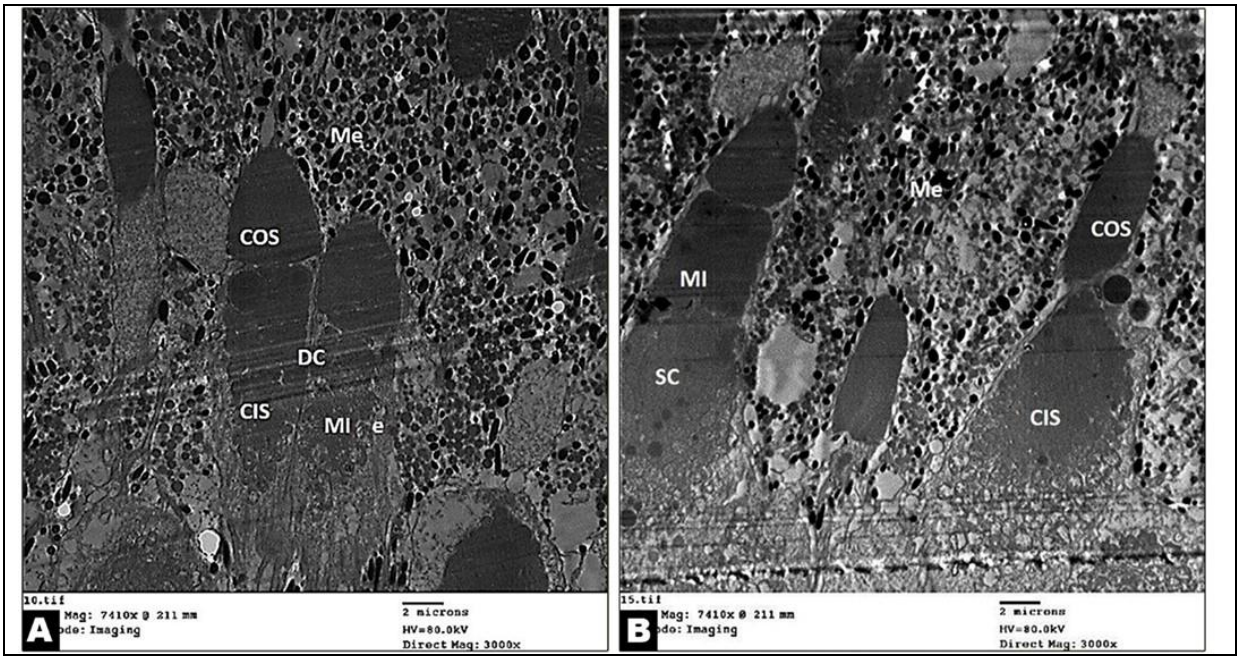

Fig. 5. Transmission electron microscopic micrographs of the retinal photoreceptor layer of Fantail goldfish; Single cone **(SC)**; Double cone **(DC)**; Ellipsoid region **(e.)**; Melanosomes **(Me)**; Mitochondria **(Mi)**; Cone outer segment **(COS)** and Cone inner segment **(CIS)**. (A and B X 3000)

DISCUSSION

The vertebrate eye is a crucial organ in numerous activities, especially the feeding behavior, which are adapted to the unique environmental conditions of each type of vertebrate. Terrestrial vertebrates have perfect vision in various air conditions; however, this vision becomes hyperopic underwater, indicating eye adaptations **(Jones *et al.*, 2007)**, while aquatic vertebrates have good underwater vision but it becomes myopic in the air **(El-Bakary & Abumandour, 2017b)**. In order to have good vision, aquatic vertebrates' eyes depend on a variety of components, such as the water's turbidity, temperature, pressure, and light-absorption mechanism. Teleost fish species in different water regions, from shallower waters to low illuminated areas, have numerous environmental optic adaptations to increase visibility in various underwater conditions **(Collin *et al.*, 2009)**.

The neighbor-joining method, initially proposed by **Saitou and Nei (1987)**, was applied to our phylogenetic relationship. This approach yielded significant findings regarding the interrelationships among *Carassius auratus*, the fantail and black moor strains. The utilization of this approach, renowned for its effectiveness and precision in managing extensive datasets, played a crucial role in clarifying the phylogenetic positions of the investigated taxa. As established by the bootstrap test (1000 repetitions), the branches inside the tree correspond to the proportion of replicate trees in which the linked taxa grouped **(Felsenstein, 1985)**. The evolutionary distances were determined with the Tamura 3-parameter approach **(Tamura, 1992)**, wherein the lengths of the branches correspond to the number of base substitutions per site. The tree is depicted on a scale. All unclear sites were

eliminated via pairwise deletion from the nine nucleotide sequences that comprised the analysis. 495 locations were included in the final dataset.

The reliability of the phylogenetic tree was deduced and was additionally enhanced through the implementation of bootstrap analysis, which adheres to the methodology advocated by **Tamura (1992)**. The high bootstrap values found in our tree provide an indication of the clustering patterns of the linked taxa being reliable. The utilization of 1000 bootstrap replicates provides this degree of assurance in the tree branches, which is consistent with the criteria established in modern phylogenetic investigations and bolsters the validity of our results. Our methodology for maintaining data integrity, particularly the elimination of uncertain positions via paired deletion, guaranteed the dependability of our dataset. While employing this approach resulted in a decrease in the quantity of positions examined (495 sites in the final dataset), it substantially improved the precision of our phylogenetic deductions. In molecular phylogenetic, this rigorous approach to data curation is critical, as it reduces the possibility of erroneous conclusions caused by faulty data.

Our histological examination of the retina in the black moor and fantail goldfish confirmed prior studies by revealing a retinal structure comparable to that of other vertebrates. An internal neural layer and an exterior pigmented epithelium (PE) are the two primary layers that make up the retina. This further subdivision of the neural layer into nine different layers is compatible with **Rodieck (1998)**. While, the basic description of the structure of vertebrate retina coincides with that previously detailed in all fish species **(Nag & Sur, 1992; Donatti & Fanta, 1999; Fishelson *et al*., 2004; Fishelson *et al*., 2012; El-Bakary & Abumandour, 2017a; Aboelnour *et al*., 2020; Cortesi *et al*., 2020; Bassuoni *et al*., 2021; Abumandour *et al*., 2022b)**.

The kind of photoreceptor—rod-shaped cells for scotopic vision or cone-shaped cells for photopic vision—and the environmental factors are correlated. Our investigation unveiled that the photoreceptor layer of both examined goldfish exclusively consists of cone cells only, a feature that is also observed in other teleost fishes, like *alestes nures* **(El-Attar *et al*., 1999)** and the zebrafish **(Allison *et al*., 2010)**. This finding may suggest that these examined fish have adapted visually to their aquatic habitat. Meanwhile, the photoreceptor layer consists of rod cells only in *A. angullia* **(Atta, 2013)**, while the observation of both rod and cone cells is the most common feature in the most teleost fish, such as the cardinal fish **(Fishelson *et al*., 2004)**, gilthead sea bream **(El-Bakary & Abumandour, 2017a)**, and golden gray mullet (*Chelon aurata*) **(Abumandour *et al*., 2022b)**. Furthermore, the presence of numerous cone cells with few rod cells is observed in the *Oreochromis niloticus* **(El-Attar *et al*., 1999)**.

An examination of the retinal photoreceptor layer in the black moor and fantail goldfish using a transmission electron microscopy reveals the singular existence of cone photoreceptor cells, which consist of both single cones (SC) and double cones (DC). This discovery is consistent with prior investigations concerning teleost fishes, which frequently have an abundance of cone photoreceptors as a result of adaptations to their visually oriented activities in aquatic habitats **(Reuter & Peichl, 2008; Allison *et al*., 2010)**. The double cones, which our research identified as comprising a main cone (CC) and an accessory cone (AC), are a distinctive feature of numerous fish species. **Caves *et al*. (2021)** hypothesized that these

structures significantly contribute to the improvement of visual acuity and color vision. The configuration of these cones, characterized by their unique outer (OS) and inner (IS) segments, conforms to the overarching structure of photoreceptors in vertebrates, as **Rodieck (1998)** has exhaustively documented.

The present findings reveal significantly that the cone cells of the photoreceptor layer in both examined goldfish have two subtypes: the single and double cone cells, similar to those observed in the golden gray mullet (*Chelon aurata*) **(Abumandour *et al.*, 2022b)**. Nevertheless, discernible distinctions can be observed in their configuration and dimensions between the two species. The black moor goldfish displays dispersed cones along this stratum, but the fantail goldfish possesses larger, more condensed cones. Similarities in the configuration and dimensions of the cones may potentially indicate divergent color perception abilities and visual acuity among the species, as hypothesized by **Lythgoe and Partridge (1989)**. However, the observations of the three subtypes of cone cells in some teleost fish but with different appearances, such as the long-single, short-single, and the double cone cells that are seen in the catfish (*Clarias batrachus*) and sardinella aurita (*Clupeidae*) **(Nag & Sur, 1992; Salem, 2016)**; the single cone and two types of the double cone cells are seen in the cardinal fish (*Apogonidae*) **(Fishelson *et al.*, 2004)**; and the single, double, and triple cone cells are seen in the gilthead sea bream (*Sparus aurata*) **(El-Bakary & Abumandour, 2017b)**. The intimate association between the outer segments of the cones and pigment epithelial cells, which we have observed, provides more evidence for their fundamental function in light absorption. The vertical and membrane-occupied configuration of these segments, which resemble flattened sacs, provides an indication of their role in light absorption and the initiation of the photo-transduction mechanism. This is consistent with the conclusions reported by **Kawamura and Tachibanaki (2008)** about the importance of the shape of the outer segment in light absorption.

The present findings reveal that the pigmented epithelium is denser and more peripherally distributed in Black Moor goldfish than in Fantail goldfish, where it covers a greater area of the photoreceptor layer. This implies the existence of a species-specific adaptation, which may be associated with variations in their habitats or behaviors, as emphasized by **Cortesi *et al.* (2020)**. This pigmented layer nearly represents $^{1}/_{3}$ of the total retinal thickness in *Sardinella aurita* **(Salem, 2016)**. This thick pigmented epithelial layer of the retina is named the non-nervous layer, as described in numerous fish, such as the rainbow trout **(Douglas, 1982)**, the European eel **(Atta, 2013)**, the flathead mullet **(El Bakary, 2014)**, the gilthead sea bream **(El-Bakary & Abumandour, 2017b)**, and the golden gray mullet **(Abumandour *et al.*, 2022a)**.

Dowling (1987) noted the purity of the outer limiting membrane as a trait that is characteristic of healthy retinal tissue in both species. The disparity in exterior nuclear layer (ENL) thickness between the two species may serve as an indicator of variations in the density of the visual cell body, potentially associated with disparities in visual processing capacity. The current findings reveal that the thickness and cell densities of the external plexiform layer (EPL) vary between species. Moreover, the fantail goldfish and the black moor goldfish display a considerably greater density of bipolar and horizontal cells inside

their outermost layers. Based on the hypothesis of **Marc and Cameron (2001)**, this difference may be indicative of distinct synaptic processing capacities in their retinas. In addition, the variations in the internal nuclear layer (INL) underscore the unique cellular compositions that characterize the two species. In contrast to the black moor goldfish, which has a more dispersed INL, the fantail goldfish has a more compact INL. This may be due to variations in their visual processing pathways, as **Dowling (1987)** suggests. With conclusion, our research indicates that the linkage between bipolar and ganglion cells differs between species in regard to the internal plexiform layer (IPL) and the ganglion cell layer (GCL). Additionally, the inner limiting membrane and nerve fiber layer (NFL) thickness exhibited variation between the two species, which may suggest disparities in the transmission of signals from the retina to the brain.

Our TEM findings revealed that the densely packed mitochondria in the ellipsoid region of the inner segments of these cones indicate a high level of metabolic activity, which is crucial for photoreceptor function. This conclusion is consistent with the findings of **El-Bakary and Abumandour (2017a)** and **Koenig and Gross (2020)**, who underscored the significance of mitochondria in meeting the metabolic requirements of photoreceptors.

CONCLUSION

The study utilized DNA barcoding, histology, and TEM analyses to explore the evolutionary connections and retinal adaptations of *Carassius auratus*, focusing on the black moor and fantail goldfish strains. Our phylogenetic investigation used the neighbor-joining approach to identify intimate connections among these strains, supported by substantial bootstrap values. Both strains exhibited a retinal structure similar to vertebrates, consisting of a nine-layered internal neural layer and an exterior pigmented epithelium. Goldfish strains have cone photoreceptors, with differences in photoreceptor arrangement and retinal thickness that may indicate varying color perception and visual acuity, possibly due to their unique ecological environments. The cones reveal specific configurations that are specifically designed to enhance light absorption and photo-transduction. Significantly, discrepancies in the thickness of the retinal layers between the fantail and the black moor indicate the unique ecological adaptations and visual processing capabilities.

Declaration statement

Ethical approval and consent to participate

This study has been carried out with ethical permission from the Faculty of Science, Al-Azhar University, and approved by the Institutional Animal Care and Use Committee. Moreover, it has been carried out with ethical permission from the Faculty of Veterinary Medicine, Alexandria University, and approved by the Institutional Animal Care and Use Committee (ALEXU-IACUC). All methods were performed in accordance with the relevant guidelines and regulations by the Basel Declaration and the International Council for Laboratory Animal Science (ICLAS).

Author contributions

All authors contributed to conceptualization, methodology, software, validation, formal analysis, investigation, resources, data curation, writing original draft preparation, writing review and editing, visualization, and supervision. **All authors** have read and agreed to the published version of the manuscript.

Acknowledgements

We thank the Faculty of Science (girls) and (boys) of Al-Azhar University and the Faculty of Veterinary Medicine of Alexandria University for their help complete this article and for providing the scanning electron microscope unit to complete the ultrastructural examinations.

REFERENCES

Aboelnour, A.; Noreldin, A.E.; Massoud, D. and **Abumandour, M.M.A. (2020).** Retinal characterization in the eyes of two bats endemic in the Egyptian fauna, the Egyptian fruit bat (*Rousettus aegyptiacus*) and insectivorous bat (*Pipistrellus kuhlii*), using the light microscope and transmission electron microscope. *Microsc. Res. Tech.*, **83**: 1391–1400.

Abumandour, M.M.A.; Bassuoni, N.F. and **Hanafy, B.G. (2021).** Ultrastructural studies of the pecten oculi of the Garganey (*Anas querquedula*, Linnaeus 1758) and the Eurasian common moorhen (*Gallinula chloropus chloropus*, Linnaeus 1758). *Microsc. Res. Tech.*, **84**: 1967-1976.

Abumandour, M.M.A.; Massoud, E.; El-Kott, A.; Morsy, K.; El-Bakary, N.; Abumandour, R.; El-Mansi, A. and **Kandyel, R. (2022b).** Morphological adaptations on the eye of the golden gray mullet (*Chelon aurata*): Using light and scanning electron microscopical study. *Microsc. Res. Tech.*, **85**: 2105-2112.

Abumandour, M.M.A.; Morsy, K. and **Hanafy, B.G. (2022a).** Biological features of the pecten oculi of the European wild quail (*Coturnix coturnix*): Adaptative habits to Northern Egyptian coast with novel vision to its SEM–EDX analysis. *Microsc. Res. Tech*., **85**: 3817-3829.

Allison, W.T.; Barthel, L.K.; Skebo, K.M.; Takechi, M.; Kawamura, S. and **Raymond, P. (2010).** Ontogeny of cone photoreceptor mosaics in zebrafish. *Journal of Comparative Neurology*, **518**: 4182-4195.

Atta, K. (2013). Morphological, anatomical and histological studies on the olfactory organs and eyes of teleost fish, *Anguilla anguilla* in relation to its feeding habits. *The Journal of Basic & Applied Zoology*, **66**: 101-108.

Azab, A.M.; Shoman, H.M.; El-Deeb, R.M.; Abdelhafez, H.M. and **Samei, S.E.A. (2017).** Comparative studies on the histology of eye retina in some Nile fishes with different dial activities. *The Egyptian Journal of Hospital Medicine*, **68**: 815-823.

Bassuoni, N.F.; Abumandour, M.M.A.; El-Mansi, A. and **Hanafy, B.G. (2021).** Visual adaptation and retinal characterization of the Garganey (*Anas querquedula*): Histological and scanning electron microscope observations. *Microsc. Res. Tech*., **85**: 607-616.

Baumel, J.J.; King, S.A.; Breazile, J.E.; Evans, H.E. and **Berge, J.C.V. (1993).** Handbook of avian anatomy: Nomina Anatomica Avium. 2nd ed. Nuttall Ornithological Club. 779p., Cambridge.

Bolasina, S.N.; de Azevedo, A. and **Petry, A.C.J.A.R. (2017).** Comparative efficacy of benzocaine, tricaine methanesulfonate and eugenol as anesthetic agents in the guppy, *Poecilia vivipara*. *Aquaculture Reports*, **6**(C): 56-60.

Braekevelt, C.R. (1994). Retinal photoreceptor fine structure in the great blue heron (*Ardea herodias*). *Anatomia, histologia, embryologia*, **23**: 281-292.

Caves, E.M.; de Busserolles, F. and **Kelley, L.A.J.c. (2021).** Sex differences in behavioural and anatomical estimates of visual acuity in the green swordtail, *Xiphophorus helleri*. *Journal of Experimental Biology*, **224**: jeb243420.

Collin, S.P.; Davies, W.L.; Hart, N.S. and **Hunt, D.M. (2009).** The evolution of early vertebrate photoreceptors. *Philo. Trans. R. Soc. Lond. B. Biol. Sci*., **364**: 2925–2940.

Cortesi, F.; Mitchell, L.J.; Tettamanti, V.; Fogg, L.G.; de Busserolles, F.; Cheney, K.L. and **Marshall, N.J. (2020).** Visual system diversity in coral reef fishes. *Seminars in Cell & Developmental Biology*, **106**: 31-42.

Darwish, S.T.; Mohalal, M.E.; Helal, M.M. and **El-Sayyad, H.I. (2015)**. Structural and functional analysis of ocular regions of five marine teleost fishes (*Hippocampus hippocampus*, *Sardina pilchardus*, *Gobius niger*, *Mullus barbatus* & *Solea solea*). *Egyptian Journal of Basic and Applied Sciences*, **2**: 159-166.

Dimech, M.; Stamatopoulos, C.; El-Haweet, A.E.; Lefkaditou, E.; Mahmoud, H.H.; Kallianiotis, A. and **Karlou-Riga, C. (2012).** Sampling protocol for the pilot collection of catch, effort and biological data in Egypt. Food and Agriculture Organization of the United Nations. EastMed Technical Documents.

Donatti, L. and **Fanta, E., (1999).** Morphology of the retina in the freshwater fish *Metynnis roosevelti* Eigenmann (Characidae, Serrasalminae) and the effects of monochromatic red light. *Revista brasileira de Zoologia*, **16**: 151-173.

Douglas, R. (1982). The function of photomechanical movements in the retina of the rainbow trout (*Salmo gairdneri*). *Journal of Experimental Biology*, **96**: 389-403.

Dowling, J.E. (1987). The Retina: An Approachable Part of The Brain. Harvard University Press.

El-Attar, A.; Al-Zahby, S. and **Atta, K. (1999).** Comparative histological and biometric studies on the olfactory organs and eyes of differently feeding fishes, *Alestes nures*, *Oreochromis niloticus* and *Bargrus bayad*. *JOURNAL-EGYPTIAN GERMAN SOCIETY OF ZOOLOGY*, **28**: 29-52.

El-Bakary, N.E.R. and **Abumandour, M.M. (2017b).** Visual adaptations of the eye of the gilthead sea bream (*Sparus aurata*). *Veterinary Research Communications*, **41**: 257-262.

El-Bakary, N.E.R. and **Abumandour, M.M.A. (2017a).** Visual adaptations of the eye of the gilthead sea bream (*Sparus aurata*). *Vet. Res. Commun*., **41**: 257-262.

El Bakary, N.E.R. (2014). Visual Adaptations of the Eye of *Mugil cephalus* (Flathead Mullet). *World Applied Sciences Journal*, **30**: 1090-1094.

Elghoul, M.; Morsy, K. and **Abumandour, M.M.A. (2022).** Ultrastructural characterizations of the pecten oculi of the common ostrich (*Struthio camelus*): New insight to scanning electron microscope–energy dispersive X-ray analysis. *Microsc. Res. Tech.*, **85**: 1654-1662.

Felsenstein, J. (1985). Phylogenies and the comparative method. *The American Naturalist*, **125**: 1-15.

Fishelson, L.; Ayalon, G.; Zverdling, A. and **Holzman, R. (2004).** Comparative morphology of the eye (with particular attention to the retina) in various species of cardinal fish (Apogonidae, Teleostei). *The Anatomical Record Part A: Discoveries in Molecular, Cellular, and Evolutionary Biology*, **277**: 249-261.

Fishelson, L.; Delarea, Y. and **Goren, M. (2012).** Comparative morphology and cytology of the eye, with particular reference to the retina, in lizard fishes (*Synodontidae, Teleostei*). *Acta Zoologica (Stockholm)*, **93**: 68-79.

Gewily, D.; Shalaby, W.; Abumandour, M.M.A.; Choudhary, O.P. and **Kandyel, R. (2024).** Pecten oculi of kestrel (*Falco tinnunculus rupicolaeformes*) and little owl (*Athene noctua glaux*): Scanning electron microscopy and histology with unique insights into SEM–EDX elemental analysis. *Microscopy research and technique*, **87**: 546-564.

Hall, M.I. and **Ross, C.F. (2007).** Eye shape and activity pattern in birds. *Journal of Zoology*, **271**: 437-444.

Hayat, M. (1986). Basic Techniques for Transmission Electron Microscopy. 2nd Edn., Academic Press, Baltimore.

Jones, M.P.; Pierce, K.E. and **Ward, D. (2007).** Avian vision: a review of form and function with special consideration to birds of prey. *Journal of Exotic Pet Medicine*, **16**: 69-87.

Kandyle, R.; El Basyouny, H.A.; Morsy, K.; Abourashed, N.M.; Madkour, N. and **Abumandour, M.M.A. (2022).** Gross, ultrastructural, and histological characterizations of pecten oculi of the glossy ibis (*Plegadis falcinellus*): New insights into its scanning electron microscope–energy dispersive X-ray analysis. *Microscopy research and technique*, **85**: 3908-3920.

Kassab, A.; Aoyama, M. and **Sugita, S. (2001).** The morphology of the iridocorneal angle in the eye of buffaloes (*Bos bubalis*): A light and scanning electron microscopic study. *Okajimas folia anatomica japonica*, **78**: 145-152.

Kawamura, S. and **Tachibanaki, S. (2008).** Rod and cone photoreceptors: molecular basis of the difference in their physiology. *Comparative Biochemistry Physiology Part A: Molecular Integrative Physiology*, **150**: 369-377.

Koenig, K.M. and **Gross, J.M. (2020).** Evolution and development of complex eyes: a celebration of diversity. *Development*, **147**: dev182923.

Kondrashev, S.; Pushchin, I.; Gatilova, S. and **Kamenev, Y. (2023).** Retinal ganglion cell topography and spatial resolution in the smelt *Hypomesus japonicus* (Brevoort, 1856). *Acta Zoologica*, **104**: 552-560.

Kumar, S.; Dhingra, A. and **Daniell, H. (2004).** Stable transformation of the cotton plastid genome and maternal inheritance of transgenes. *Plant molecular biology*, **56**: 203-216.

Land, M.F. and **Nilsson, D.E. (2002).** Animal Eyes: Oxford University Press, New York.

Letunic, I. and **Bork, P. (2021).** Interactive Tree Of Life (iTOL) v5: an online tool for phylogenetic tree display and annotation. *Nucleic acids research*, **49**: W293-W296.

Levine, J.S. and **MacNichol, E.F. (1982).** Color vision in fishes. *Scientific American Inc*., **246**(2): 140-149.

Lythgoe, J. and **Partridge, J. (1989).** Visual pigments and the acquisition of visual information. *Journal of Experimental Biology*, **146**: 1-20.

Marc, R.E. and **Cameron, D. (2001).** A molecular phenotype atlas of the zebrafish retina. *Journal of neurocytology*, **30**: 593-654.

Masland, R.H. (2012). The neuronal organization of the retina. *Neuron*, **76**: 266-280.

Nag, T. and **Sur, R. (1992).** Cones in the retina of the catfish, *Clarias batrachus* (L.). *Journal of Fish Biology*, **40**: 967-969.

Peter-Ajuzie, I.; Nwaogu, I.; Majesty-Alukagberie, L.; Ajaebili, A.; Farrag, F.; Kassab, M.; Morsy, K. and **Abumandour, M. (2021).** Ocular morphology of the fruit bat, *Eidolon helvum*, and the optical role of the choroidal papillae in the megachiropteran eye: a novel insight. *Folia morphologica*, **81**: 715–722.

Ptito, M.; Bleau, M. and **Bouskila, J. (2021).** The Retina: A Window into the Brain. *Cells*, **10**: 3269.

Reuter, T. and **Peichl, L. (2008).** Structure and Function of the Retina in Aquatic Tetrapods". Sensory Evolution on the Threshold: Adaptations in Secondarily Aquatic Vertebrates, edited by J. G. M. "Hans" Thewissen and Sirpa Nummela, Berkeley: University of California Press, 2008, pp. 149-172., pp. 149-172.

Rodieck, R.W. (1998). The First Steps in Seeing. Oxford University Press, 562 pp.

Saitou, N. and **Nei, M. (1987).** The neighbor-joining method: a new method for reconstructing phylogenetic trees. *Molecular biology evolution*, **4**: 406-425.

Salem, M.A. (2016). Structure and function of the retinal pigment epithelium, photoreceptors and cornea in the eye of *Sardinella aurita* (Clupeidae, Teleostei). *The Journal of Basic & Applied Zoology*, **75**: 1 - 12.

Sanes, J.R. and **Masland, R.H. (2015).** The types of retinal ganglion cells: current status and implications for neuronal classification. *Annual review of neuroscience*, **38**: 221-246.

Shekhar, H.; Panigrahi, P. and **Sahoo, H. (2023).** Nanotechnology in Retinal Drug Delivery. In: Nanotechnology in Ophthalmology. Elsevier, Academic Press, pp.: 181-196.

Skomal, G. (1996). Goldfish. 2nd edition, Wiley Publishing Inc., 144 pp.

Suvarna, S.K.; Layton, C. and **Bancroft, J.D. (2013).** Bancroft's Theory and Practice of Histological Techniques,Expert Consult: Online and Print,7: Bancroft's Theory and Practice of Histological Techniques. Churchill Livingstone. Churchill Livingstone Elsevier.

Tamura, K. (1992). Estimation of the number of nucleotide substitutions when there are strong transition-transversion and G+ C-content biases. *Mol. Biol. Evol*., **9**: 678-687.

Veilleux, C.C. and **Kirk, E.C. (2014).** Visual acuity in mammals: effects of eye size and ecology. *Brain Behavior Evolution*, **83**: 43-53.

Wang, F.Y.; Tang, M.Y. and **Yan, H.Y.J. (2011).** A comparative study on the visual adaptations of four species of moray eel. Vision Research, **51**(9): 1099-1108.

Ward, R.D.; Zemlak, T.S.; Innes, B.H.; Last, P.R. and **Hebert, P.D. (2005).** DNA barcoding Australia's fish species. *Philosophical Transactions of the Royal Society B: Biological Sciences*, **360**: 1847-1857.

Zeigler, H.P. and **Bischof, H.J. (1993).** Vision, Brain, and Behavior in Birds. MIT Press.

Zeng, H. and **Sanes, J.R. (2017).** Neuronal cell-type classification: challenges, opportunities and the path forward. *Nature Reviews Neuroscience*, **18**: 530-546.